

Broad-Spectrum Stress and Vibration Analysis of Large Composite Container

Adrian Jensen

Predictive Engineering, Inc.

George Laird

Predictive Engineering, Inc.

Adrian Tayne

ECS Case, Becklin Holdings, Inc.

Abstract

A large composite shipping container was analyzed for drop, impact, PSD random vibration and general stress analysis. The main shell of the container was a glass-fiber vacuum infused composite with closures made of aluminum. Lifting rings and other major structural load points were attached to the composite container using thick aluminum plates with preloaded bolts to distribute point loads into the shell.

*The uniqueness of this work was that one base model could address progressive composite failure whether under static conditions (implicit) or during drop test analysis (explicit) along with bolt preload and extensive nonlinear contact behavior at closures, skid plates and load rings. Analysis recommendations are provided for general implicit analysis for: (i) PSD random vibration with bolt preload; (ii) progressive failure of composites with *MAT_54; (iii) contact modeling and (iv) optimization of run times using MPP LS-DYNA[®]. The explicit analysis of the container was rather simplistic but some comments will be made about the analysis setup and runtimes.*

Introduction

Fiberglass composites are used in a broad array of consumer goods given their reasonable mechanical properties and more importantly, low cost. Although carbon fiber rules in many applications where cost is not a consideration, fiberglass is still the industry workhorse. In this study, we discuss our analysis experience with the design of a large (1.5x3x10m) lightweight transportation container (see Figure 1 for an example of such a container). The uniqueness of this work is that we take the reader from the development of the composite property cards from manufacturer's data to experimental correlation (sandwich and solid laminates) to idealization of the structure into a highly efficient FEA model that can be used for a broad array of analysis requirements from static to PSD to drop testing.



Figure 1 – Example of large composite transportation container

Material Modeling

The container uses a mix of laminate schedules but whenever the design allows, thick solid laminates (>5mm) are replaced with sandwich laminates. Figure 2 shows an example of the sandwich with a transition zone toward the solid laminate. This composite structure is manufactured using a vacuum infusion process [1].

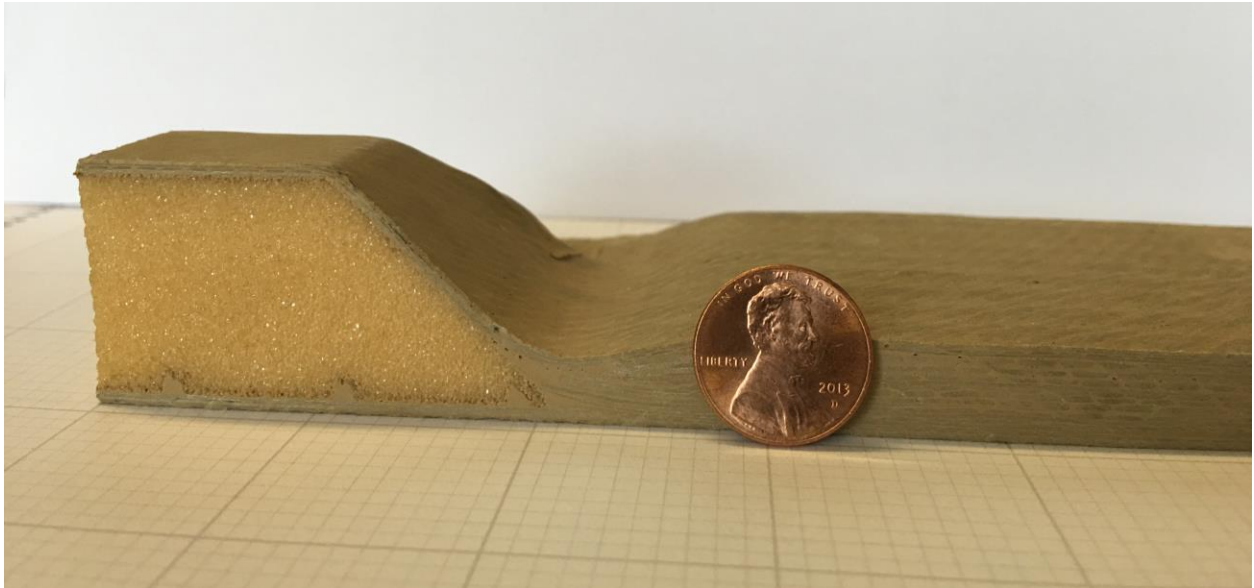


Figure 2 – Sandwich and solid laminate composites along with a transition region

We wish we could say that after exhaustive study and comparative work, we chose MAT_54 as our material model but reality is much simpler. The literature seems to like MAT_54 [2-5] and given its apparent simplicity, we went with the common denominator. The MAT_54 card was populated using vendor supplied data for the fiber given a generic plastic. Table 1 provides a summary of the vendor data for the plies and foam core used in the analysis (see Appendix for an example data sheet from the manufacturer).

Table 1 – Example Mechanical Properties of Composite Materials

| | | | | |
|---|------------|-----------|-----------|-------------|
| Weight | 1.0 oz/ft2 | 24 oz/yd2 | 24 oz/yd2 | 71.5 oz/yd2 |
| Fiber Volume Fraction (%) | 44 | 52 | 52 | 45 |
| Laminate Thickness (inch) | 0.02 | 0.024 | 0.024 | 0.084 |
| Elastic Properties | | | | |
| Young’s Modulus E ₁₁ (ksi) | 1,100 | 3,480 | 3,960 | 3,350 |
| Young’s Modulus E ₂₂ (ksi) | 1,100 | 3,480 | 3,860 | 3,360 |
| Shear Modulus, G ₁₂ (ksi) | 420 | 470 | 660 | 550 |
| Poisson’s Ratio, ν ₁₂ | 0.31 | - | - | - |
| Strength Properties | | | | |
| Tensile Strength, σ _{t11} (ksi) | 14.2 | 65.9 | 75.0 | 57.9 |
| Tensile Strength, σ _{t22} (ksi) | 14.2 | 65.9 | 75.0 | 63.6 |
| Compressive Strength, σ _{c11} (ksi) | 14.2 | 65.9 | 73.0 | 49.4 |
| Compressive Strength, σ _{c22} (ksi) | 14.2 | 65.9 | 73.0 | 46.9 |
| Shear Strength (in-plane) σ ₁₂ (ksi) | 9.81 | 9.40 | 13.0 | 7.50 |

These properties were then morphed into MAT_54 cards as given in Figure 3. The first card represents a two ply layer having a total thickness of 0.024in (0.6mm) while the second card represents four fiber layers and has a thickness of 0.084in (2.13mm). Failure strains were calculated based on the failure stress divided by the elastic modulus. Although differences were noted in tensile versus compressive failure stresses, for simplicity the same strains were used to limit data entry errors.

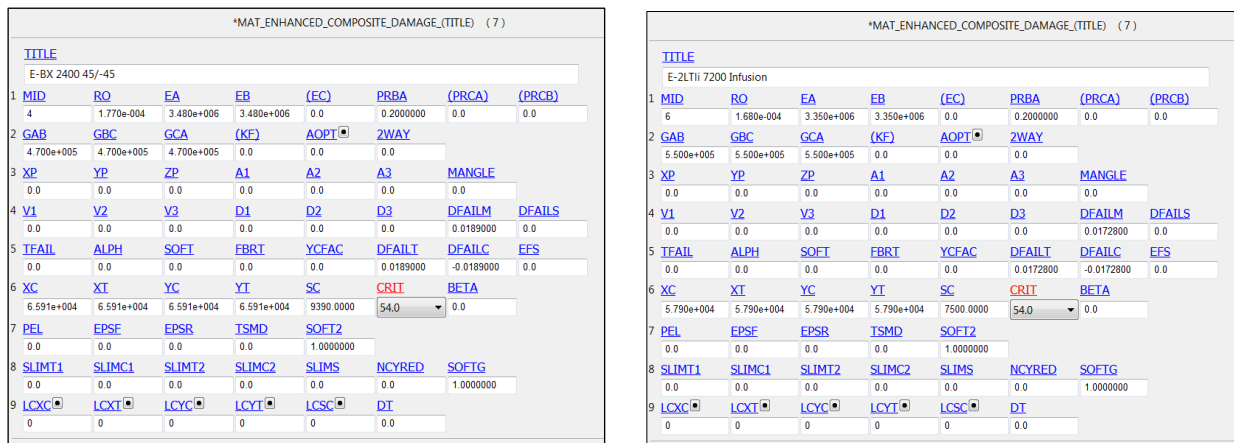


Figure 3 – MAT_54 cards for example composite materials

The Divinycell H100 foam material was similarly modeled using MAT_54 for the sandwich plate layup. For the 3D sandwich simulation, *MAT_181 was used with an estimated uniaxial compression / tension curve. These material models are given in Figure 4. In MAT_181, the foam formulation is triggered when a non-zero PR/BETA value is used.

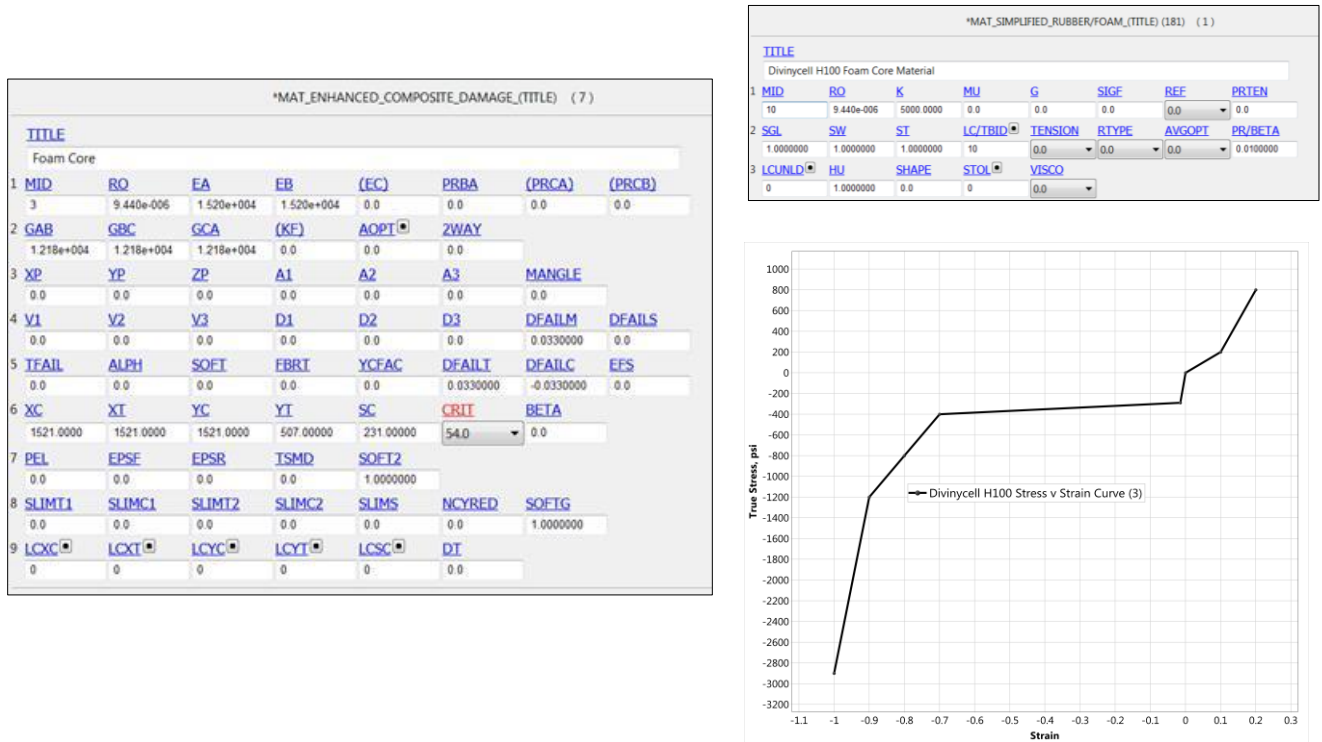


Figure 4 – MAT_54 and MAT_181 formulations for the foam core material

The material cards were then configured into layup schedules using FEMAP (general purpose FEA tool) from Siemens PLM Software. Figure 5 shows an example layup schedule. Ply 1 is at the bottom of the plate with 8 at the top surface as determined by the plate normals’.

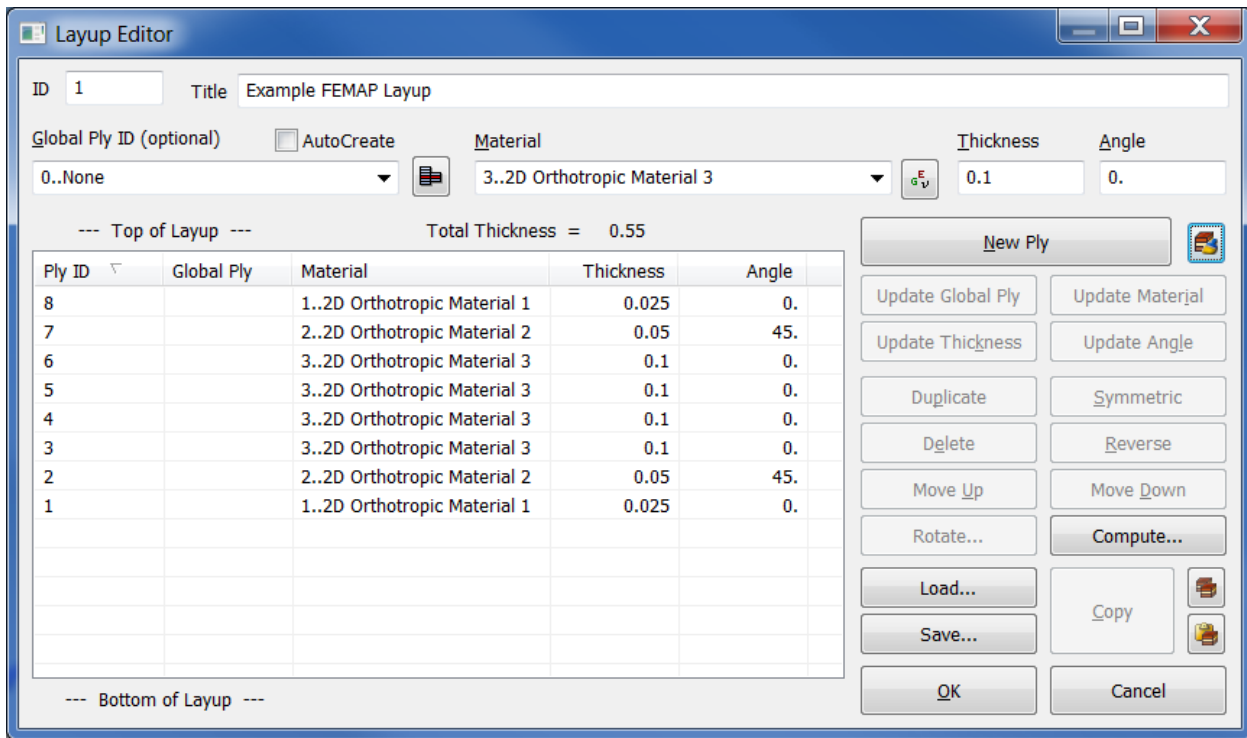


Figure 5 – Example solid laminate composite layup schedule

To validate the material cards, experimental tests were conducted on sandwich and solid laminate composites. Figure 6 shows the work conducted for the sandwich composite. All dimensions and results are in English units. The graph provides a comparison between test data, an isotropic hand calculation, the 2D plate sandwich model and then the 3D solid-plate sandwich model. To our surprise, the 2D plate formulation was significantly different than that for the 3D model. In review of the test results, one of our colleagues noted that the failure mode for the sandwich laminate was due to localized buckling under the anvils. This type of failure is not captured in the 2D plate formulation since no out-of-plane strain is calculated.

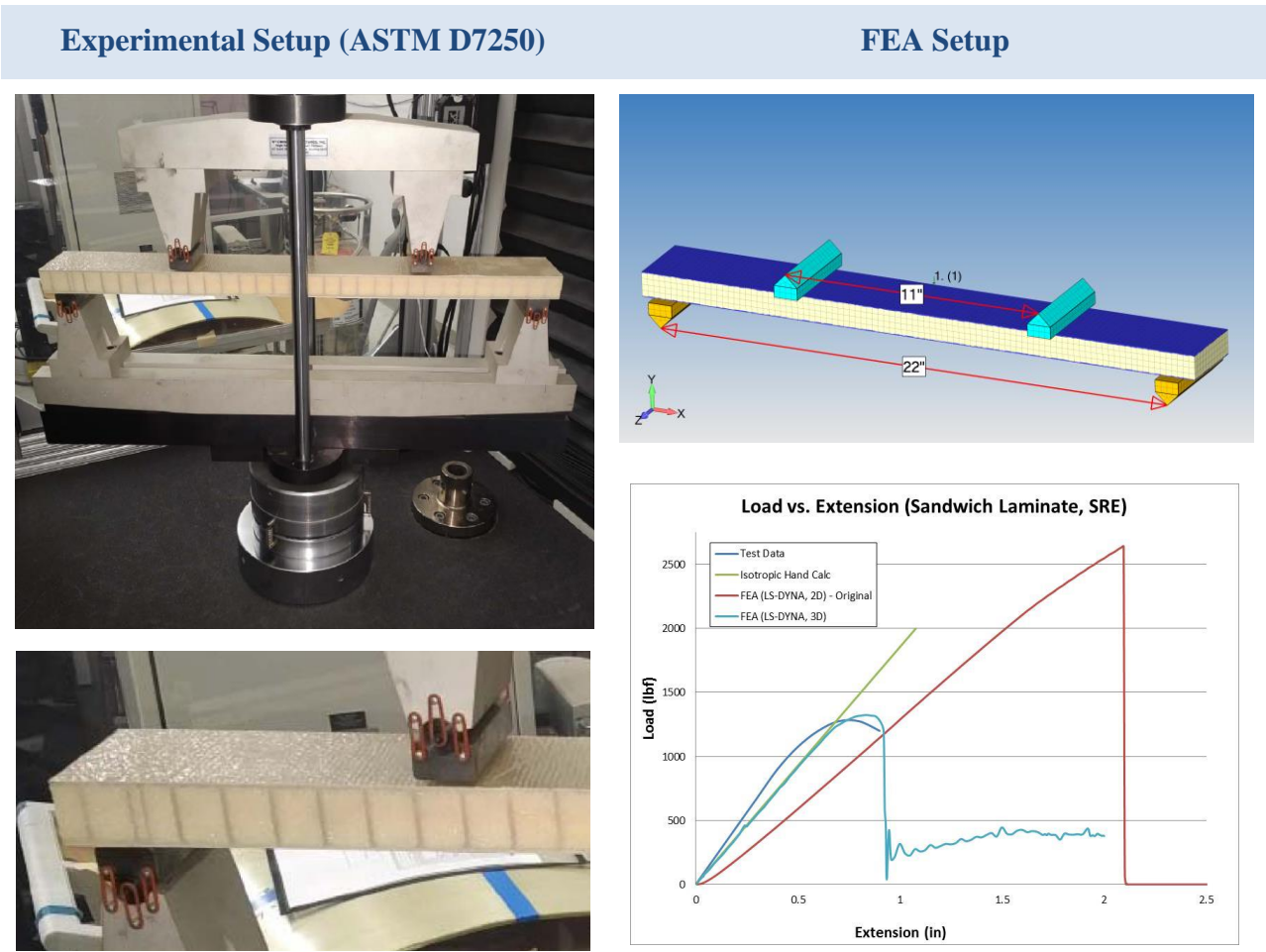


Figure 6 – Experimental work on sandwich laminate composite with FEA comparison

Figure 7 shows the failed sandwich composite from testing. The failure mode is induced by buckling of the skin due to localized softness of the foam directly under the anvil. The FEA model using out-of-the-box manufacturer’s data correlated to the precision of the test (+/- 10%). The model was analyzed using LS-DYNA’s implicit solver (MPP double-precision). It is unknown as of this writing as to how such a failure behavior could be captured using a 2D plate laminate model. It should be noted that this failure mechanism is unique to this test method and that in general engineering structures where the load is diffuse (e.g., pressure loading) or under general bending and tension, the 2D and 3D formulations should converge and provide approximately the same results. Given this caveat, the authors don’t wish to mislead the reader and claim that all sandwich composite structures must be modeled using a 3D formulation only that the model should fit the application or in this case, the test.

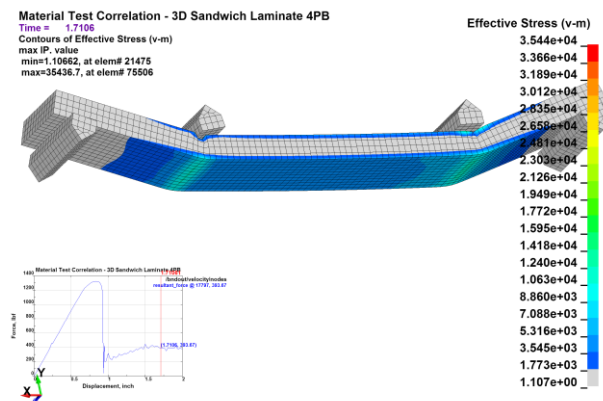
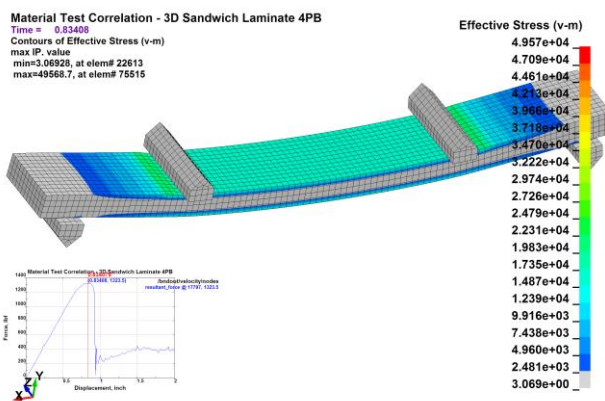
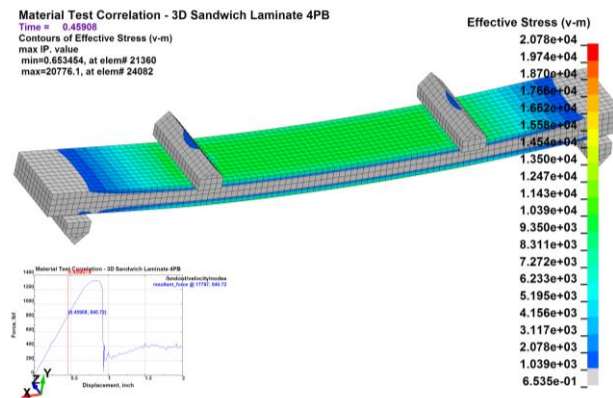


Figure 7 – 3D sandwich laminate composite failure analysis

For the solid laminate it was very low drama and the 2D plate model lined up spot-on with the test results as shown in Figure 8.

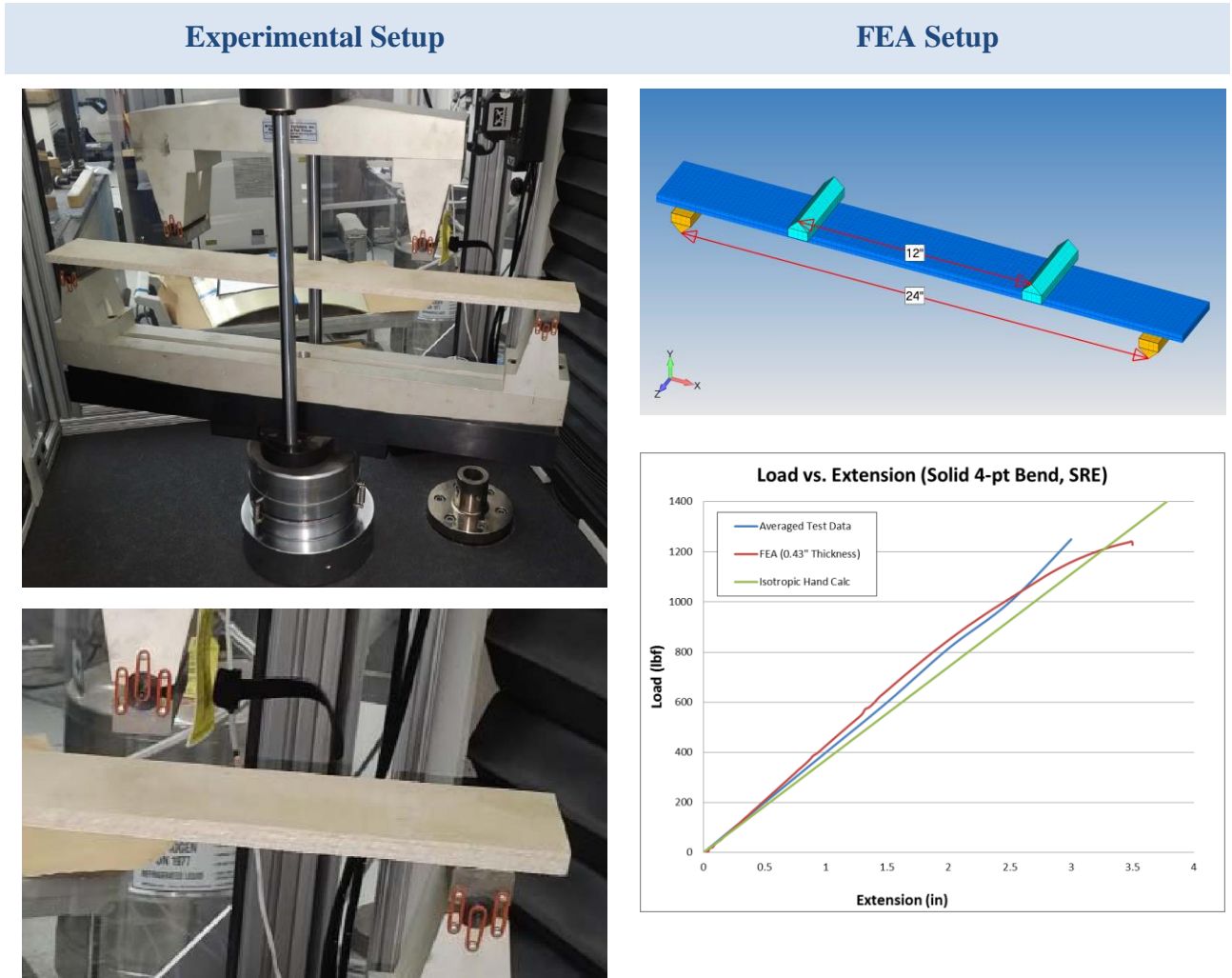


Figure 8 - Experimental work on solid laminate composite with FEA comparison

Finite Element Model of Large Composite Container

The FEA model was idealized from 3D solid geometry into mid-plane surface geometry using FEMAP. This skin geometry was then meshed to create a reasonably uniform quad-dominant mesh as shown in Figure 9. The model uses plates, solids, beams, cables, discrete-beams, spotweld, mass and CNRB. Aluminum reinforcement components and skid plates are attached to the container via preloaded bolts (ELFORM=9 w/ *MAT_100).

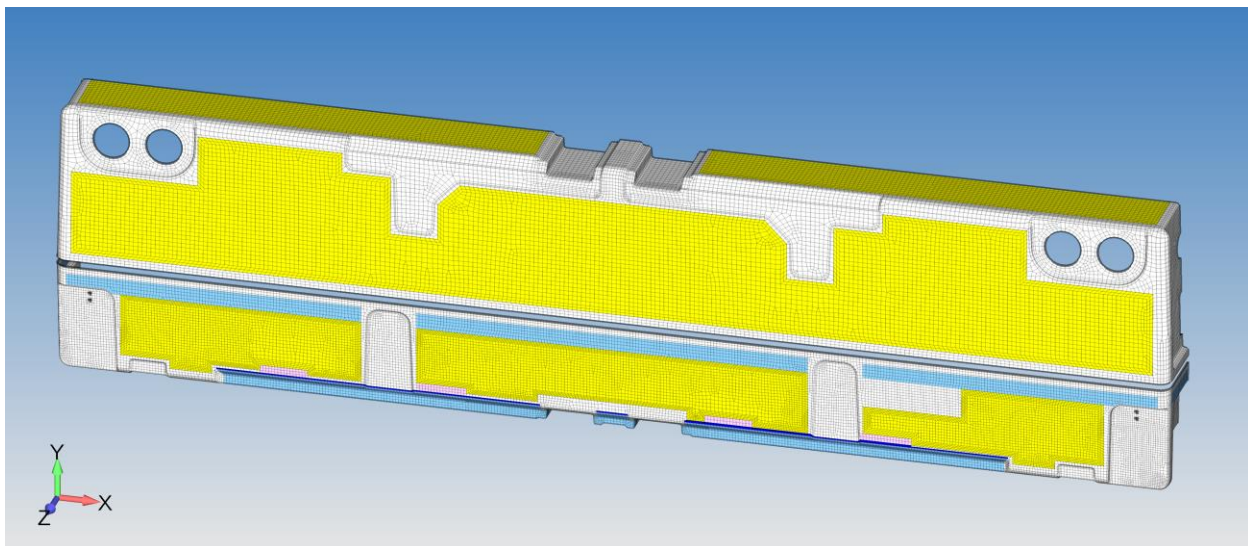
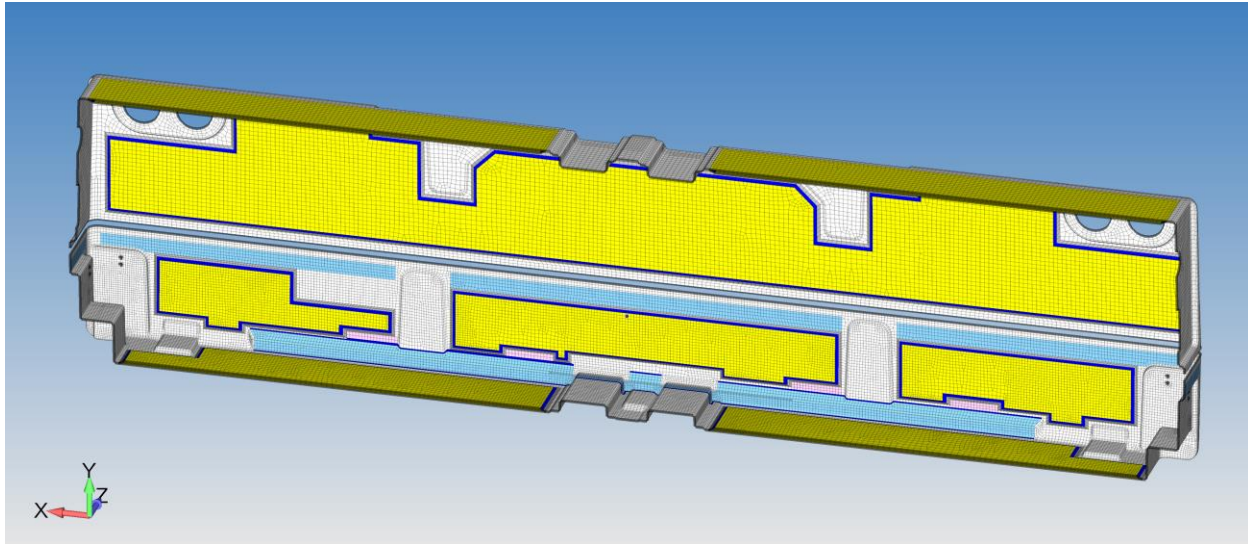


Figure 9 – FEA model of large composite container

Only the largest penetrations were modeled in detail for the container where it was known that high stresses would occur due to impact loading. Figure 10 provides a few details on the mesh paving used on the model. Given that the model was going to be run in explicit, the aimed time step was 1 μ s. With a nominal composite wave speed of 3500 m/s, element sizes could be as small as 3.5 mm if needed, but in general, the mesh sizing was set to 25 mm. The model contains 150k elements and 125k nodes.

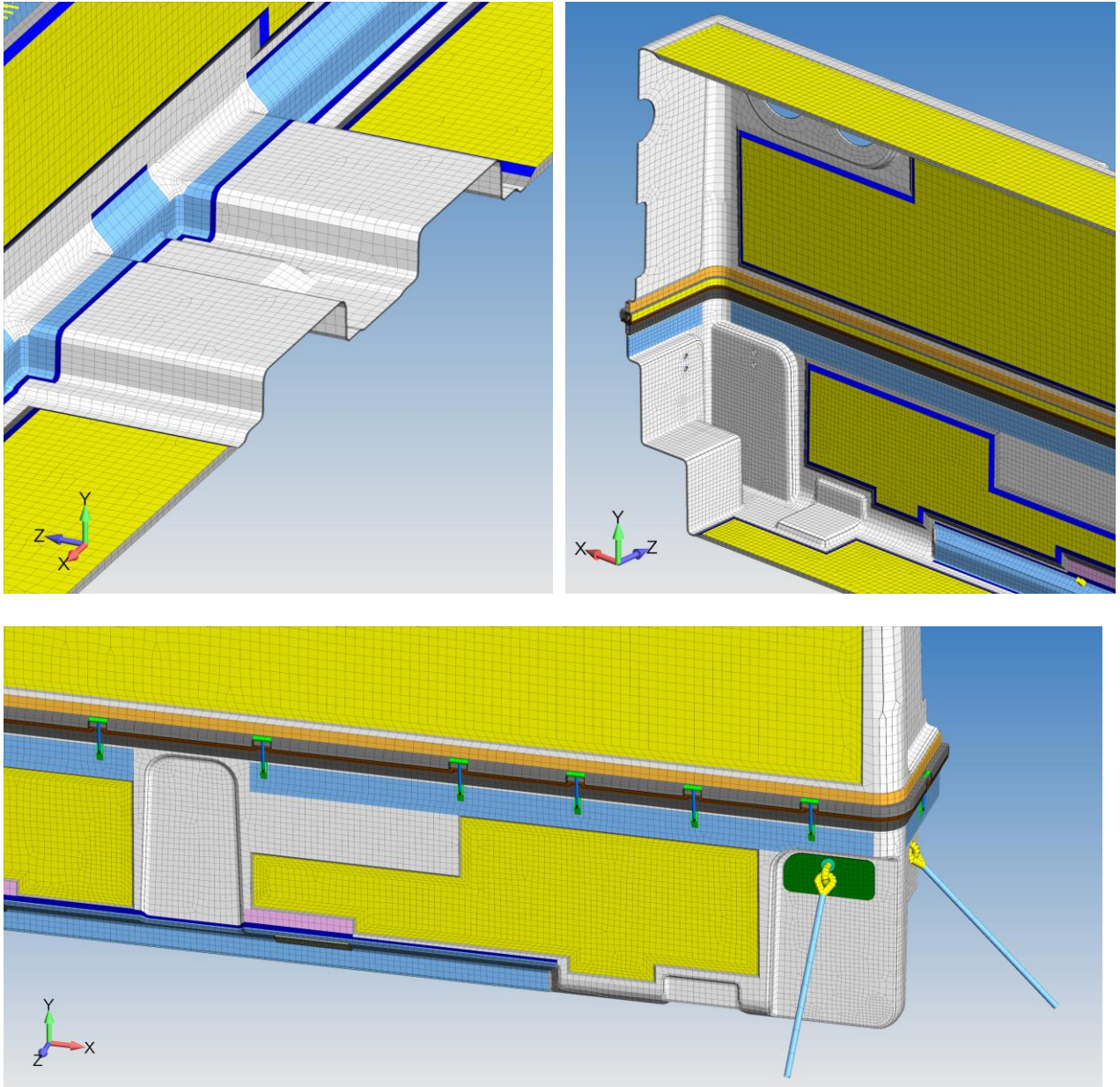


Figure 10 – Details of mesh construction used for the container

Implicit and Explicit Setup and Analysis Techniques

In general, implicit settings were leveraged from recommendations from DYNAmore [6-7]. From our perspective over the years, the single biggest improvement has been in contact via the implementation of mortar contact [8-9]. Of course, the complete list of improvements is extensive and the reader is recommended to read the most recent draft version of the LSTC Keyword Manual. A brief technical note on implicit is also available from Laird [13]. The material models used for implicit and explicit are given in Table 2 with a brief explanation on how they were used. The same material setup was used as the model was switched between implicit and explicit.

Table 2 – Material Models Used For Implicit and Explicit Analyses

| N° | Title | Usage |
|-----|-------------------------------------|--|
| 000 | MAT_ADD_EROSION | To differentiate compressive versus tensile failure modes in metallic materials [10]. |
| 001 | MAT_ELASTIC | Materials of non-structural interest. |
| 020 | MAT_RIGID | Material idealization of impact surface (e.g., concrete). |
| 024 | MAT_PIECEWISE_LINEAR_PLASTICITY | Workhorse material law for aluminum and steel components that can plastically deform during loading. |
| 054 | MAT_ENHANCED_COMPOSITE_DAMAGE | Sandwich skin and solid laminates |
| 067 | MAT_NONLINEAR_ELASTIC_DISCRETE_BEAM | Idealization of shock isolation mounts using nonlinear force / deflection response with damping. |
| 071 | MAT_CABLE_DISCRETE_BEAM | Latch, lift and tie-down cables. |
| 100 | MAT_SPOTWELD | Bolt preload for latches, bolted attachments to container and general fasteners. |
| 181 | MAT_SIMPLIFIED_RUBBER/FOAM | Foam core of sandwich laminate composite. |

Element formulations were simpler and Table 3 provides a description of what was used and if the formulation was switched between implicit and explicit.

Table 3 – Element Types and Formulations for Implicit and Explicit Analyses

| Type | Title | Usage | ELFORM N° | |
|----------|----------------|---|-----------------|----------|
| | | | Implicit | Explicit |
| Beam | SECTION_BEAM | Bolts and latch fastening hardware. | 1 | 1 |
| Beam | SECTION_BEAM | Discrete beam and cable for nonlinear spring and cable latches, lifting and tie-down cables. | 6 | 6 |
| Beam | SECTION_BEAM | Bolt preload (paired with MAT_100). | 9 | 9 |
| Shell | SECTION_SHELL | Thin and rangy metallic structures used for structural reinforcement of the container and the closure. | 16 | 2 |
| Solid | SECTION_SOLID | Thick metallic structures and foam core of sandwich composite. | -1 | 1 |
| Laminate | PART_COMPOSITE | All composite structures from the sandwich skin to the solid laminate. The shell formulation was set to ELFORM=16 | 16 ¹ | 16 |

¹The current recommendation is ELFORM=-16 for implicit but we got good results with the standard.

LS-DYNA Solver Selection

For implicit, our recommendation is to go with double-precision and MPP. The use of double-precision is somewhat required for solution convergence one can sneak by occasionally with single-precision but even it converges one should check it with double-precision. As for SMP versus MPP, the mortar contact algorithm is optimized for MPP and it is our understanding that the future belongs to MPP and we should embrace it. Now we have the conundrum of whether to use a release version (e.g., R8.1.0) or a current development (dev) version. Given how rapidly the implicit solver has been changing, it can be advantageous to start with a dev version. For this work reported here, we used the dev version 106595, MPP double-precision. However, please keep in mind that it is our understanding that dev versions are not fully tested or optimized and that surprises may be in store for the analyst. Putting some meat behind this comment, we were working with this prior dev version and noticed that it gave 30% higher failure loads in our validation work against test results. Through some digging and providing the LSTC team with our test data, it was determined that the dev version had some errors. Of course it was quickly corrected but it was quite a detour through the weeds. As any simulation engineer realizes, it is a far cry from a cartoon to a validated simulation and we are often working on the edge.

Contact Settings Implicit and Explicit

For implicit, there is only mortar contact of interest [8, 9]. For beam-to-beam contact, the `SINGLE_SURFACE_MORTAR` contact has worked well and in general we have strived to use this formulation for all general contacts and when needed for model debugging employ `FORCE_TRANSDUCER` cards to extract contact forces. For mortar contact with neat interfaces (i.e., no interpenetration), default settings are recommended. When tied interfaces are required to idealize welded or simplistic bolted connections, it is recommended by Grimes [7] to use the `_CONSTRAINED_` option to avoid numerical difficulties via the standard penalty method for tying interfaces together. In this work, we were able to just use the `TIED_NODES_TO_SURFACE_OFFSET` formulation.

In the case of explicit, we continued to use Mortar contact with acceptable performance on our models that ranged from 200k to 400k nodes and elements. This simplified the process of automatically (within the same analysis run) switching between implicit and explicit. For example, all PSD and explicit runs had an initial implicit preload sequence and thus avoiding the process of setting up birth/death for a passel of contacts or setting up a `SENSOR` routine.

Implicit Control Cards

Solution settings for implicit control are given in Table 4 along with an explanation of why they were needed or recommended by others [5-7, 9 & 11]. In Table 4, only those fields that were changed from the default are discussed. In many cases, we will say “RTM” (read the manual) and we are always referring to the latest draft release of the Keyword User’s Manual and we will only list other references when such information is not contained within the User’s Manual.

Table 4 – Implicit Control Cards for Composite Analysis with Plasticity and Contact

| Keyword | Fields Changed | Explanation |
|--------------------|---|--|
| _ACCURACY | OSU=1 & IACC=1 | RTM |
| _CONTACT | SSTHK=1 | IGNORE=-1 is new and deals with how Mortar contact handles single-surface contact and additional information is in the manual. SSTHK=RTM |
| _IMPLICIT_AUTO | IAUTO=1 & DTMAX=-5 | IAUTO=RTM while DTMAX=RTM it is worth mentioning how clever LSTC is at times with their usage of fields. The negative number refers to curve where key points (fixed solution outputs) are requested. In this manner, one can has your solution kick out D3PLOT states at specific times and/or change your DTMAX setting. |
| _IMPLICIT_DYNAMICS | IMASS=1, GAMMA=0.6 & BETA=0.38 | Although these settings are covered in the Keyword Manual one should also read DYNAmore’s Implicit User Guide [6]. Extremely useful Keyword for getting implicit models to run. |
| IMPLICIT_GENERAL | IMFLAG=1 | RTM |
| _SHELL | LAMSHT=1 | RTM – a strong recommendation for laminate composites |
| IMPLICIT_SOLUTION | NSOLVR=12, ABSTOL=1e-20 & NLPRINT=2 | These settings were arrived at by trial and error and of course, starting from a basis provided by DYNAmore references [6, 9 & 11]. We started with the defaults for DCTOL, ECTOL and RCTOL paired with ABSTOL=1e20. This provided acceptable solution convergence as of this writing. |

On the use of CONTROL_IMPLICIT_DYNAMICS, one may ask why it is present within a nonlinear static analysis. We have found that it stabilizes contact during initialization and when modeling progressive failure in laminate composites, it facilitates rapid convergence by allowing ply layers to fail gracefully. As for adding unwanted dynamic effects, the recommended settings of GAMMA=0.6 and BETA=0.38 provide sufficient numerical damping that the authors have not noticed any deleterious dynamic effects within the range of models and loads studied in the past several years. Typically we strive to quietly apply loads and keep the time range within a second (1.0).

Explicit Control Cards

There is nothing out of the norm in our settings for explicit since it is the “bread and butter” for LS-DYNA. We would like to mention the ever-prevalent, little-commented use of `BULK_VISCOSITY` in LS-DYNA decks by the pros. Although the Keyword Manual states that its use is for attenuating the effects of shock wave propagation in a numerical model, it appears as a standard Keyword entry for non-shock analysis. Bali [12] provides a good explanation of its usage and recommends the default settings of `q1=1.5` and `q2=0.06`. The only modification is to use `type=-2` to include shells in the calculation. The other settings for `_CONTACT` and `_TIMESTEP` are routine. Table 5 provides a synopsis of the Keyword cards used within the explicit analysis routine.

Table 5 – Explicit Control Cards

| Keyword | Fields Changed | Explanation |
|------------------------------|---------------------------------|--|
| <code>_BULK_VISCOSITY</code> | <code>TYPE=-2</code> | This setting enables the application to shells and is not the default. |
| <code>_CONTACT</code> | <code>SSTHK=1</code> | RTM |
| <code>_HOURLASS</code> | <code>IHQ=8 & QH=0.1</code> | This was found to be particular useful for the <code>ELFORM=16</code> composite shells. It was noted that during some analyses elements would “die” unexpectedly. This stopped once <code>IHQ=8</code> was employed. Although better element quality most likely could have prevented the use of this hourglass formulation it is unknown at this writing. |
| <code>_TIMESTEP</code> | <code>DT2MS=-1.6667e-6</code> | Mass scaling to shorten run time. |

Modeling Practices and Results

Implicit Analyses

Nonlinear Static Stress Analysis

The bulk of the simulation effort was done as nonlinear static. An idea of the load cases are: pseudo-rail impact (LOAD_BODY_), decompression and sealing pressure loads (LOAD_SEGMENT), lifting and transportation loading (more LOAD_BODY_) and just all sorts of other cases that uses a combination of _BODY, _SEGMENT & _NODE_. Many components in the structure were attached to the composite container via bolted connections. These bolted connections were preloaded (INITIAL_AXIAL_FORCE_BEAM) and with contact friction enabled, various built-up sections of aluminum shielding, lifting hooks and composite laminate could be squeezed together to simulate the manufactured state. It was a bit amazing how well it worked once the model was debugged.

Several the load cases were very challenging to the structure and dozens of runs were required. Scaling of the implicit solution was pivotal in helping us get the project done. Figure 11 shows results from the rail impact load case along with how it scales under MPP Double-Precision.

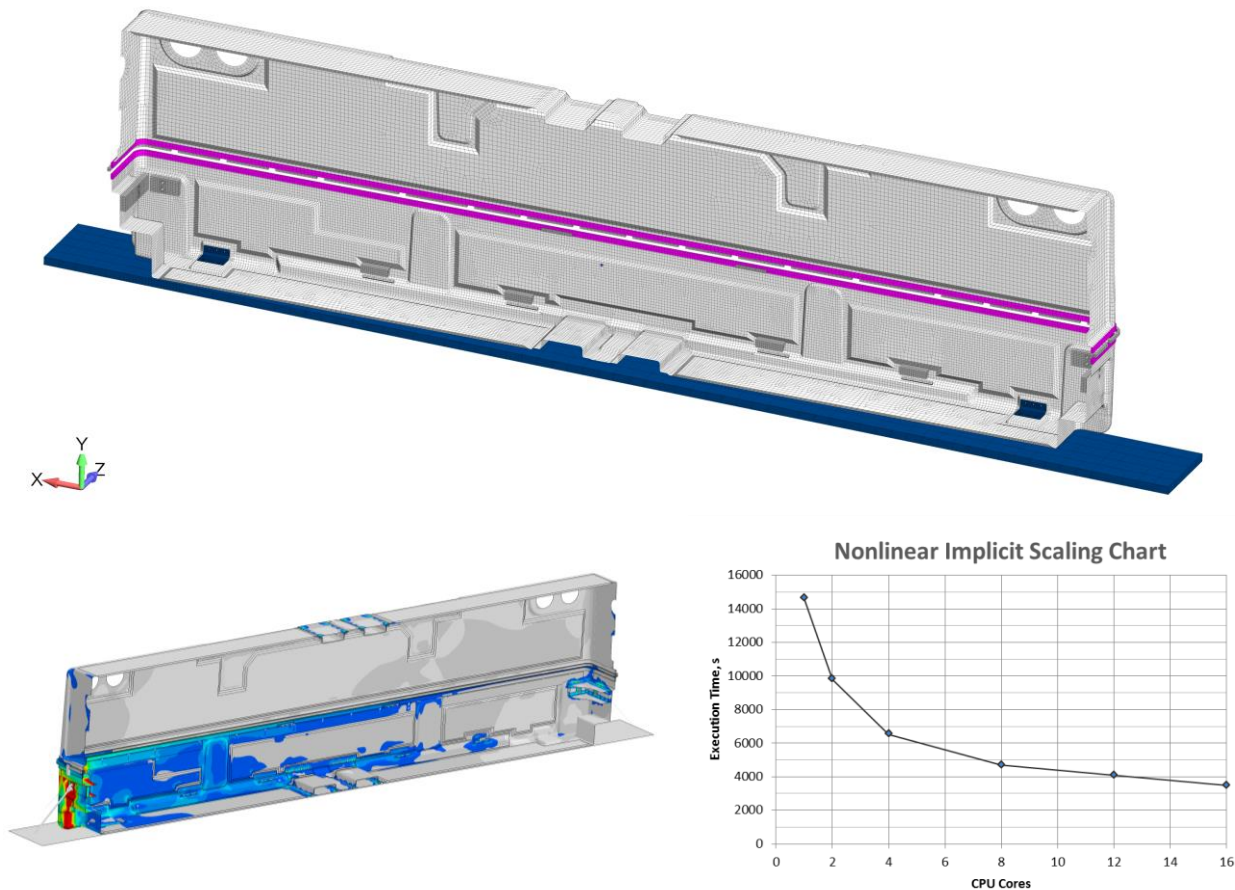


Figure 11 – Nonlinear static analysis of rail impact with MPP scaling results

Eigenvalue and PSD Analyses

If your model is setup to run dynamic implicit, then it is a one card addition to request an eigenvalue analysis (CONTROL_IMPLICIT_EIGENVALUE). This is no big deal but the real utility of an Eigenvalue (normal modes) analysis comes to the forefront when combined with a nonlinear implicit analysis and is setup using a negative number on the NEIG field where the number is a curve ID that defines the time to perform an eigenvalue analysis and the number of modes to calculate. Normal modes or Eigenvalue analysis is the foundation for a whole-host of frequency domain solutions from modal frequency (e.g., shaker table sin-sweep analysis) to seismic to NVH to PSD. LS-DYNA can perform all of these solutions [14-16] with acceptable scaling [17].

Although the intermittent Eigenvalue analysis was very useful in debugging the container model, our design requirement was to perform a PSD analysis under road, rail and air transport using MIL-STD-810G. To avoid having to run multiple PSD runs, we enveloped the PSD 810G spectra and then analyzed the worst case in the orthogonal directions. Figure 12 shows the model used in this analysis (no symmetry) along with the enveloped PSD curve. To ensure that we were capturing the worst-case behavior, we removed tiedowns from the opposing side of any excited direction to leave only one side connected. Additionally and uniquely, we first ran a nonlinear static analysis first to preload the bolted connections and the reinforcement sections and to seat the container latch system. Once the model was in the transport condition, it was hit with the PSD. This was done all within one analysis sequence with no restart.

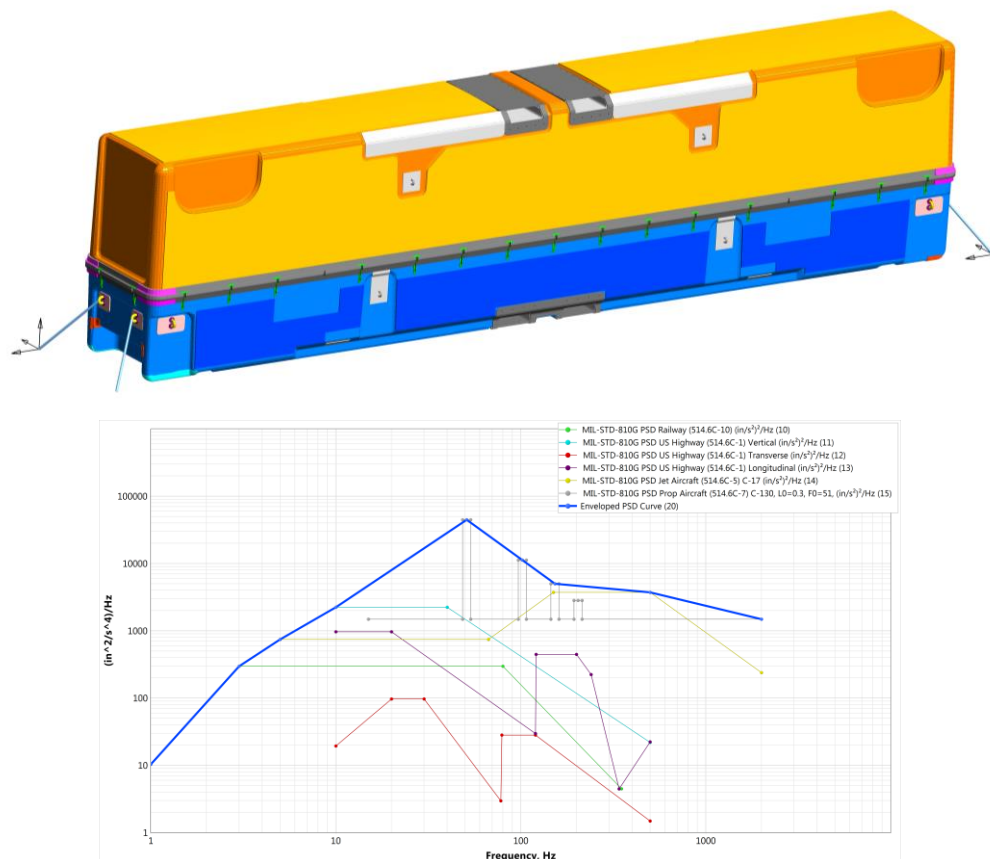


Figure 12 – PSD analysis of composite container showing enveloped PSD curve

The setup for the PSD analysis is covered in the Keyword Manual but is a bit brief. The baseline Keywords are from Table 4 and then the cards given in Table 6 are added to the deck. Only the fields that were modified from default are shown. The NEIG=-4 calls out the curve to initiate the Eigenvalue analysis to extract 50 normal modes at time=0.10 while the MSTRESS=1 requests that stresses are generated for the PSD analysis. To activate the PSD analysis, one inserts the FREQUENCY_DOMAIN_RANDOM_VIBRATION card. In this analysis we requested that it sum modal results up 2000 Hz with 2% damping. The PSD method was base acceleration (VAFLAG=1). The other fields are explanatory via the manual. It should be mentioned that the technique applies the PSD excitation through BOUNDARY_SPC's that have DOFZ=1 (DOF=3). In Nastran one often uses a multi-point constraint (MPC) to tie together the base nodes and then excite this MPC in the desired direction. The field LDPSD=20 merely calls out the curve that defines the PSD excitation. As with any classic PSD technique one needs to be mindful of units. The authors would recommend that for your first foray into this solution technique that one builds a simple model and verify it against a known solution or something out of Steinberg [18].

Table 6 – Nonlinear Implicit PSD Analysis Control Cards

| *CONTROL_IMPLICIT_EIGENVALUE | | | | | | | | |
|------------------------------------|--------|--------|-----|-------|--------|-------|------|--|
| Card | NEIG | | | | | | | |
| 1 | -4 | | | | | | | |
| | | | | | MSTRES | | | |
| 2 | | | | | 1 | | | |
| *FREQUENCY_DOMAIN_RANDOM_VIBRATION | | | | | | | | |
| Card | | | | FNMAX | | | | |
| 1 | | | | 2000 | | | | |
| | DAMPF | | | | | | | |
| 2 | 0.02 | | | | | | | |
| | VAFLAG | METHOD | | | VAPSD | VARMS | NPSD | |
| 3 | 1 | 1 | | | 1 | 1 | 1 | |
| 4 | | | | | | | | |
| | SID | | DOF | LDPSD | | | | |
| 5 | 1 | | 3 | 20 | | | | |

Results from the PSD analysis were nothing unusual and the standard RMS-von Mises plots can be generated at the end of the analysis routine. It should be mentioned that one also has access to all the Eigenvector results through LSPP along with modal effective mass information in the eignout file. For the design work, the technique work extremely well and the analysis sequence scaled well under MPP. Figure 13 provides a glimpse at the principal eigenvector in the Z-direction along with the RMS von Mises stress and an idea of how this solution sequence scales using the LS-DYNA MPP double-precision solver.

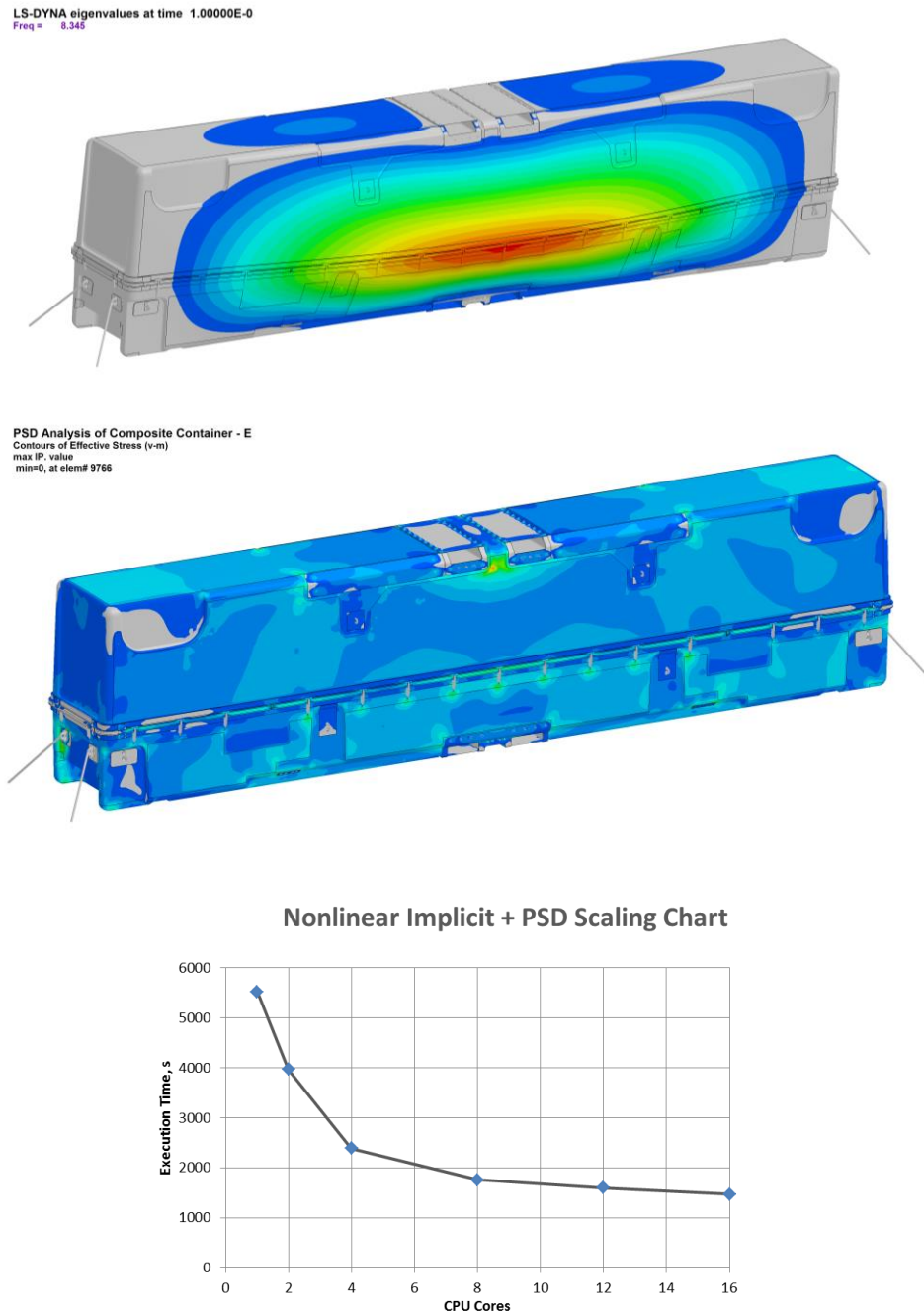


Figure 13 – Characteristic PSD stress results and implicit frequency solution sequence scaling chart

Explicit Analysis

Given that the model was built for both implicit and explicit work, it was mostly a housekeeping task to translate the model. It should be mentioned that if speed wasn't important, the model could run out-of-the-gate in explicit mode. As covered in Table 2 and Table 3, the process is direct and simple. Given the ability to run the majority of the load cases as nonlinear implicit, only the drop case required an explicit solution.

Figure 14 shows the setup for the drop test onto the long edge of the container. The model had 370k nodes and 320k elements.

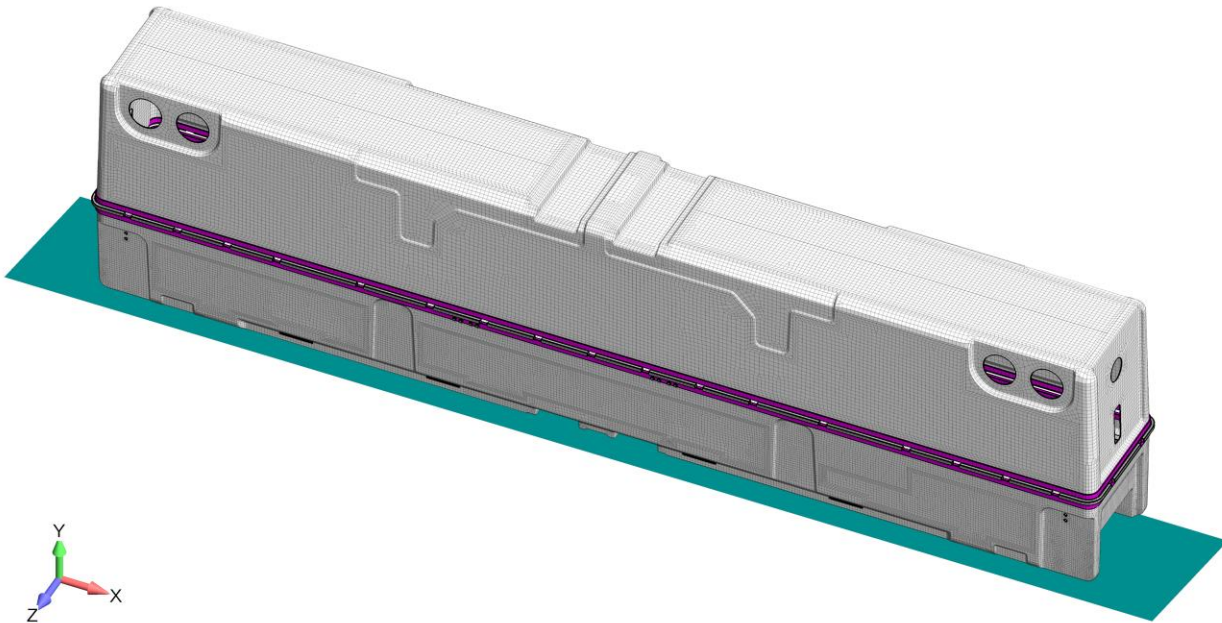
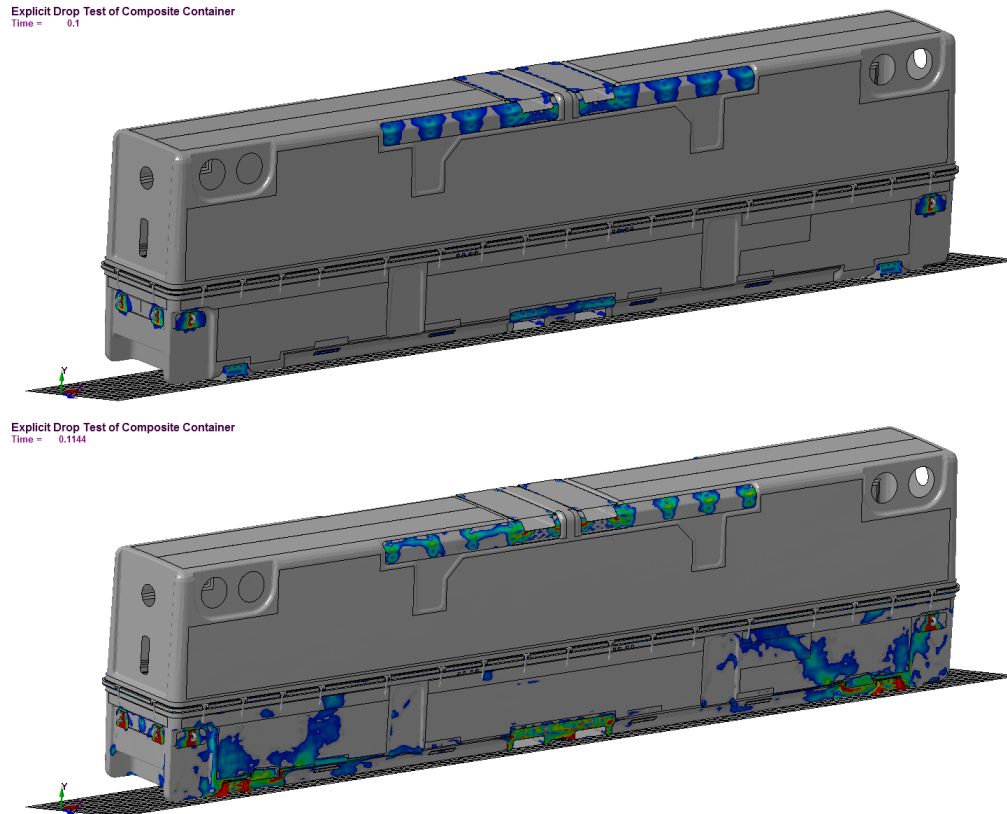


Figure 14 – Explicit simulation of drop impact analysis of composite container

The initial velocity setup for this edge drop can be done in a variety of ways. The concept is that the container is resting on its far edge, nine inches above a hard surface and then drops. The container rolls and then smacks the hard edge as idealized by a rigid surface. The initial velocity setup was done by using `INITIAL_VELOCITY_GENERATION`. To set preload of latches, bolted connections and gravity, the analysis started in implicit and then was switched to explicit once the container was settled. Given that an implicit preload analysis was done first, the initial velocity application was delayed through the use of `INITIAL_VELOCITY_GENERATION_START_TIME`. This delayed start then required the use of two initial velocity Keyword cards with one using `Phase=1` and the second with `Phase=0`. Why two cards are required is not well understood by the authors.

Results from this drop test and scaling results for the implicit and explicit run are given in Figure 15. The top image shows the preload state prior to initial velocity initialization while the second image shows the impact stresses. Scaling is as with prior work.



Nonlinear Implicit + Explicit Drop Test
Scaling Chart

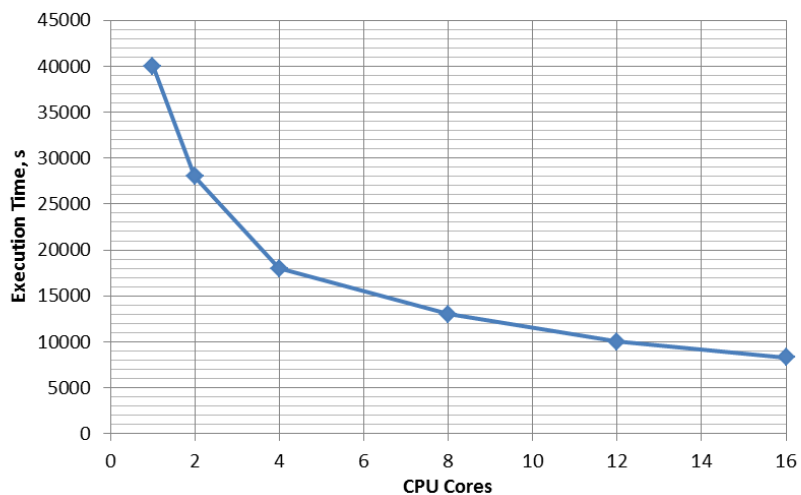


Figure 15 – Bolt Preload following by impact stresses and implicit/explicit scaling results

Summary

Nonlinear implicit mechanics in LS-DYNA have rapidly advanced in the last decade and has opened doors into more efficient solutions of complex problems. We hope that this work has demonstrated how one can leverage the nonlinear implicit solution sequence to solve commercially relevant problems in the field of composite mechanics.

Author's Note

At first glance, it may appear that a lot of LS-DYNA usage is tribal and restricted to only those that have slain the dragon; the reality is that with a little research and thoughtful use of existing technical resources within LSTC and DYNAmore, all is pretty well laid out for the novice to become an expert. We have tried within this note to provide clear references to how we have learned to do implicit and if the interested reader would like, one can find the LS-DYNA deck (minus the confidential nodes/elements) at www.predictiveengineering.com/content/project-overview. We would also welcome to hear about your experiences with LS-DYNA implicit and would encourage you to contact us and perhaps we might have a suggestion or two to get your model up and running.

Acknowledgements

Without the kind and generous technical support from the team at LSTC (Jim, Satish, Thomas, Todd, Yun and Roger), we most likely would be still spinning our numerical wheels getting this project done. We would also like to thank Dr. John Hallquist for hiring such great people within the LSTC organization that went above and beyond in helping us with this project. Our sponsor for this work was ECS Case of Grants Pass, OR. They were great colleagues to have on this numerical adventure, and through their support, they facilitated some of the best work that the authors have done in nonlinear mechanics.

References

- [1] Paepegem, W.V., Mechanics of Composite Materials, www.composites.urgent.be, Vacuum Infusion – The Equipment and Process of Resin Infusion, 2015.
- [2] Andersson, M. et al, Crash Behavior of Composite Structures, Chalmers University of Technology, Goteborg, Sweden, 2014.
- [3] Wade B., Feraboli, P. and Rassaian, M., LS-DYNA MAT54 for Simulation Composite Crash Energy Absorption, JAMS 2011.
- [4] Wade. B. and Feraboli, P., Composite Damage Material Modeling for Crash Simulation: MAT54 & the Efforts of the CMH-17 Numerical Round Robin, JAMS 2014 Technical Review.
- [5] Day, J., Erhart, T. and Hartmann, S., LSTC Composite Notes for MAT54_MAT55, 2015.
- [6] Jonsson, A. and Lilja, M. Some Guidelines for Implicit Analyses Using LS-DYNA, DYNAmore, 2014.
- [7] Grimes, R., A Tutorial on How to Use Implicit LS-DYNA, 12th International LS-DYNA User's Conference, 2012.
- [8] Borrvall, T., Mortar Contact for Implicit Analysis, LS-DYNA Forum, Ulm, 2012
- [9] Borrvall, T., A Guide to Solving Implicit Mortar Contact Problems in LS-DYNA, DYNAmore Nordic AB Technical Note.
- [10] Laird, G., LS-DYNA: Observations on Material Modeling, FEA Information, January 2016.
- [11] Borrvall, T., Experimental Nonlinear Implicit Solver 12 in LS-DYNA, DYNAmore Nordic AB Technical Note.
- [12] Bali, S., Bulk Viscosity for Shells and Solids in LS-DYNA, <http://www.d3view.com/bulk-viscosity-for-shells-and-solids-in-ls-dyna/>, January 2007.
- [13] Laird, G., Observations on Implicit Modeling, FEA Information, August 2015.
- [14] Huang, Y, et al., Mode-based Frequency Response Function and Steady State Dynamics in LS-DYNA, 11th International LS-DYNA Conference, 2010.
- [15] Rassaian, M. et al, Structural Analysis with Vibro-Acoustic Loads in LS-DYNA, 10th International LS-DYNA Conference, 2008.
- [16]
- [17] Laird, G., Large Scale Normal Modes and PSD Analysis with Nastran and LS-DYNA 12th International LS-DYNA Conference, 2012.
- [18] Steinberg, D., Vibration Analysis for Electronic Equipment, 3rd Edition (or any edition for that matter), 2000.